

See discussions, stats, and author profiles for this publication at: <https://www.researchgate.net/publication/7774583>

Polypeptide Multilayer Films: Role of Molecular Structure and Charge

ARTICLE *in* LANGMUIR · JUNE 2004

Impact Factor: 4.46 · DOI: 10.1021/la036330p · Source: PubMed

CITATIONS

69

READS

33

5 AUTHORS, INCLUDING:



Kiran Chakravarthula

VNR Vignana Jyothi Institute of Engineering...

5 PUBLICATIONS 71 CITATIONS

SEE PROFILE

Polypeptide Multilayer Films: Role of Molecular Structure and Charge

Donald T. Haynie,^{*,†,‡} Shantanu Balkundi,[†] Naveen Palath,[§]
Kiran Chakravarthula,[†] and Komal Dave[†]

Biomedical Engineering, Physics, and Chemical Engineering, Institute for
Micromanufacturing, Louisiana Tech University, P.O. Box 10137, Ruston, Louisiana 71272

Received December 10, 2003. In Final Form: February 15, 2004

The role of molecular structure, charge, and hydrophobicity in polyelectrolyte layer-by-layer assembly (LbL) of thin films has been studied using the model polypeptides poly-L-glutamic acid (PLGA) and poly-L-lysine (PLL), quartz crystal microbalance (QCM), and circular dichroism spectroscopy (CD). The adsorption behavior of PLGA and PLL has been compared with the structure of these molecules in aqueous solution under the same conditions. The data show that the deposition of polypeptide per adsorption step scales with average secondary structure content, whether α helix or β sheet. This is contrary to the expectation based on the view that hydrogen bonds are crucial to polypeptide film assembly, because secondary structure formation in a polypeptide reduces its intermolecular hydrogen-bonding potential. The data also show that polypeptide adsorption scales with ionic strength and chain length. Taken together, the results increase knowledge of polypeptide-based LbL thin film fabrication and will help to provide a firmer foundation for the use of natural or designed polypeptides in LbL.

Introduction

Formation of a thin film by alternate dipping of a charged surface into dilute solutions of a polycation and a polyanion is popularly known as layer-by-layer assembly (LbL).¹ This area of research has been studied extensively during the last 10 years, both experimentally (e.g., refs 2–14) and theoretically (e.g., ref 15). In LbL, polyelectrolyte complexes can be fabricated one molecular layer at a time; it is possible to create a highly uniform multilayer thin film of precisely controlled thickness and “architecture.” The LbL approach has been used to study a broad range of polyelectrolytes, including proteins (reviewed in ref 16), and interest in LbL has risen sharply on finding that combinations of ionic attractions and repulsions lead

to structures of intriguing and potentially quite useful physical properties (reviewed in ref 17).

Most researchers in this field have used strong polyacids and polybases, meaning that the linear charge density is essentially 1 and fixed. A minority, however, have investigated physical properties of thin films made of weak polyelectrolytes, for instance, Rubner and colleagues. These researchers have used poly(acrylic acid) (PAA) and poly(allylamine hydrochloride) (PAH) to fabricate multilayer films of controlled layer thickness and molecular organization by adjusting the pH of the dipping solutions.^{18,19} A solution buffered at a certain pH will determine the average linear charge density of the adsorbing polymers pH and influence the charge density of the film surface. Control of pH thus enables control of the blending of polyanions and polycations at the molecular level.

LbL films can also be produced by hydrogen bonding. Stockton and Rubner, for example, have shown that polyaniline adsorbs to certain nonionic, water-soluble polymers because they contain groups that can form hydrogen bonds with polyaniline at amine and imine sites.²⁰ The thickness of a bilayer of such a system can be controlled at the molecular level. Understanding the molecular origin of the adsorption process will suggest ways in which LbL can be exploited in technological applications.²¹

In this work we have used PLL and PLGA to investigate the role of molecular structure and charge in polypeptide LbL. These polymers have been chosen as a model of what could be done in LbL with biologically interesting polypeptides. Analysis of their behavior could also provide insight into the physics of LbL. Our approach was to use

* To whom correspondence should be addressed.

[†] Biomedical Engineering.

[‡] Physics.

[§] Chemical Engineering.

(1) Decher, G. *Science* **1997**, *277*, 1232–1237.

(2) Cooper, T. M.; Campbell, A. L.; Crane, R. L. *Langmuir* **1995**, *11*, 2713–2718.

(3) v. Klitzing, R.; Möhwald, H. *Langmuir* **1995**, *11*, 3554–3559.

(4) Hoogeveen, N. G.; Cohen Stuart, M. A.; Fleer, G. J. *Langmuir* **1996**, *12*, 3675–3681.

(5) Krasemann, L.; Tieke, B. *Langmuir* **2000**, *16*, 287–290.

(6) Brynda, E.; Houska, M.; Wikerstal, A.; Pientka, Z.; Dyr, J. E.; Brandenburg, A. *Langmuir* **2000**, *16*, 4352–4357.

(7) Mendelsohn, J. D.; Barrett, C. J.; Chan, V. V.; Pal, A. J.; Mayes, A. M.; Rubner, M. F. *Langmuir* **2000**, *16*, 5017–5023.

(8) Ruths, J.; Essler, F.; Decher, G.; Riegler, H. *Langmuir* **2000**, *16*, 8871–8878.

(9) Clark, S. L.; Hammond, P. T. *Langmuir* **2000**, *16*, 10206–10214.

(10) Shimakazi, Y.; Nakamura, R.; Ito, S.; Yamamoto, M. *Langmuir* **2001**, *17*, 953–956.

(11) Dai, J.; Jensen, A. W.; Mohanty, D. P.; Erndt, J.; Bruening, M. L. *Langmuir* **2001**, *17*, 931–937.

(12) Picart, C.; Lavalle, P.; Hubert, P.; Cuisinier, F. J. G.; Decher, G.; Schaaf, P.; Voegel, J.-C. *Langmuir* **2001**, *17*, 7414–7424.

(13) Dubas, S. T.; Schlenoff, J. B. *Langmuir* **2001**, *17*, 7725–7727.

(14) Büscher, K.; Graf, K.; Ahrens, H.; Helm, C. A. *Langmuir* **2002**, *18*, 3585–3591.

(15) Castelnovo, M.; Joanny, J.-F. *Langmuir* **2000**, *16*, 7524–7532.

(16) Lvov, Y. In *Protein Architecture: Interfacing Molecular Assemblies and Immobilization Biotechnology*; Lvov, Y., Möhwald, H., Eds.; Marcel Dekker: New York, 2000; pp 125–167.

(17) *Multilayer Thin Films: Sequential Assembly of Nanocomposite Materials*; Decher, G., Schlenoff, J. B., Eds.; Wiley-VCH: Weinheim, Germany, 2003; 524 pp.

(18) Yoo, D.; Shiratori, S.; Rubner, M. F. *Macromolecules* **1998**, *31*, 4309–4318.

(19) Shiratori, S. S.; Rubner, M. F. *Macromolecules* **2000**, *33*, 4213–4219.

(20) Stockton, W. B.; Rubner, M. F. *Macromolecules* **1997**, *30*, 2717–2725.

(21) Lowack, K.; Helm, C. A. *Macromolecules* **1998**, *31*, 823–833.

CD for analysis of polymer structure in solution and QCM for analysis of film assembly. Far-UV CD is remarkably sensitive to the backbone conformation of polypeptides; it generally reflects the secondary structure content of a peptide. QCM detects minute mass changes (~ 10 ng) as the frequency change of an electrode. The experimental data show a marked relationship between polyelectrolyte structure in solution and adsorption behavior: the greater the amount of secondary structure in solution, the greater the amount of polymer deposited per adsorption cycle. The results constitute an analysis of the relationship of polyelectrolyte structure in solution and a study in comparison and contrast to recent closely related work.^{12,22–28}

Given the great potential of substituting polypeptides for polyelectrolytes such as PAA and PAH, particularly in applications where biocompatibility is a chief design concern, it is surprising that so few papers have been published on polypeptide LbL. The results will be of general interest to LbL researchers, because they shed further light on the molecular basis of the multilayer film assembly process, and to LbL researchers concerned with biomaterials development, drug delivery, and chiral separations.²⁹

Materials and Methods

Polypeptide Solutions. Polypeptide chains have a linear topology. Lyophilized preparations of PLGA and PLL were procured from Sigma-Aldrich, Inc. All peptides were stored at -20 °C prior to use, dissolved in aqueous solution, and introduced into a filtration device of molecular weight cutoff well below the average mass of the peptides. The concentration of the peptides was then increased by centrifugation and reduced by adding fresh solvent; this process was repeated at least 3 times to "rinse" the peptides. Peptide preparations were assessed by reversed-phase high-performance liquid chromatography and found to be polydisperse, as expected; solution-phase synthesis yields a polydisperse product. Variables of interest were chain length (λ), charge per unit length (λ), ionic strength (I), and average secondary structure content. The average molecular masses of the peptides in the length-dependence study were 1500–3000 Da (PLGA, "small"), 3800 Da (PLL, "small"), 17 000 Da (PLGA, "medium"), 48 100 Da (PLL, "medium"), 50 300 Da (PLGA, "large"), and 222 400 Da (PLL, "large"). Charge per unit length was adjusted by buffering the solution at pH 4.2 (10 mM citric acid-sodium citrate), 7.3 or 7.4 (10 mM Tris), or 10.5 (10 mM sodium carbonate) and adjusting the pH with concentrated HCl or NaOH. Ionic strength was adjusted using NaCl. For the ionic strength and pH studies the average molecular masses were 84 600 Da (PLGA) and 84 000 Da (PLL). This corresponds to ca. 655 residues each and a contour length of ca. 238 nm. Polypeptide concentration was determined by peptide bond absorbance using an extinction coefficient of $2.711 \text{ L} \cdot (\text{g} \cdot \text{cm})^{-1}$ at 221 nm;³⁰ at this wavelength absorbance is approximately independent of secondary structure content.³¹

Circular Dichroism Spectroscopy. CD enables determination of the structure of chiral molecules by detection of the differential absorption of right- and left-circularly polarized light. In the far-UV region of the spectrum, 180–260 nm, the signal is highly sensitive to the average conformation of the polypeptide backbone. The peptide concentration was $0.05 \text{ mg} \cdot \text{mL}^{-1}$. The temperature was 23 °C. Twenty (length dependence and pH dependence) or fifty scans (ionic strength dependence) of each sample were collected in a quartz cell of 0.1 cm path length, using a Jasco J-810 spectropolarimeter (Japan) with 100 mdeg sensitivity, 1 nm bandwidth, 1 s response time, 1 nm data pitch, and $100 \text{ nm} \cdot \text{min}^{-1}$ scanning rate. The scans were averaged. Buffer baselines were determined with the same instrument settings and subtracted from the respective sample spectra. Raw CD data were converted to mean molar residue ellipticity.

Spectral Deconvolution. The CDPro software suite,³² which includes three popular methods for estimating the secondary structure content of a sample from CD spectra—CDSSTR, CONTIN/LL, and SELCON3—was used to deconvolute far-UV CD spectra into contributions from α helix, β sheet, β turn, and coil. The reference set consisted of the far-UV CD spectra of 43 proteins of known secondary structure content. Further details of the similarities and differences of the CDSSTR, CONTIN/LL, and SELCON3 algorithms are discussed in ref 32 and references therein. The principle of deconvolution is discussed below.

Quartz Crystal Microbalance. Multilayer thin film assembly of PLGA and PLL at room temperature was monitored by QCM (Agilent 53131A 225 MHz universal counter). This method enables sensitive determination of mass deposited during adsorption. Each resonator was composed of a thin quartz plate less than 1 mm thick, both sides sputtered with silver (Sanwa Tsusho Co., Ltd, Japan). The nominal resonant frequency was 9 MHz. Resonator frequency, f , decreased in proportion to the mass of material adsorbed, m . In this case $\Delta f \approx -\Delta m(1.83 \times 10^8)/A$, where the surface area of the resonator $A \approx 0.16 \pm 0.01 \text{ cm}^2$ (ref 16 and references therein). The mass sensitivity constant, $1.83 \times 10^8 \text{ Hz} \cdot \text{cm}^2 \cdot \text{g}^{-1}$, enabled calculation of the mass of deposited polypeptide. In the present work only the relative amount of deposited material was chiefly relevant, and this is reflected equally well by f , Δf , or Δm . The polypeptide concentration was $2 \text{ mg} \cdot \text{mL}^{-1}$ in each case; during adsorption the volume occupied by each polymer in solution was a cube ca. 41 nm on a side (somewhat less than 20% of the contour length). The procedure used for film preparation was as follows: (1) Prepare solutions of PLL and PLGA as described above; (2) Carry out alternating immersion of the QCM resonator in these solutions for 20 min; (3) After each adsorption step, rinse the resonator for 1 min in deionized water; (4) Dry the resonator in a stream of gaseous nitrogen; (5) Monitor the deposition of material by QCM.

Results

pH and Conformation. Figure 1a displays CD spectra of PLGA and PLL in aqueous solution as a function of pH. The buffer concentration was 10 mM. At pH 7.3, where $\lambda \approx 1$, PLGA and PLL were in largely disordered, coil states, while at pH 4.2 and 10.5, respectively, PLGA and PLL were in largely helical states (Table 1). In both cases, however, PLGA was the more structured polymer; the negative Cotton effect near 195 nm, indicative of irregular backbone structure, was more negative for PLL than PLGA, and the negative Cotton effect in the range 210–225 nm, characteristic of helical backbone structure, was more negative for PLGA than PLL. Figure 1b shows the adsorption of PLGA and PLL at constant chain length (the average contour length was 238 nm), and low ionic strength. Helical PLGA adsorbed more extensively than helical PLL. Adsorption showed a substantial dependence on amount of secondary structure (or λ). In general, the amount of mass deposited per adsorption step was higher in the more-ordered but less highly charged conformation

(22) Cheng, Y.; Corn, R. M. *J. Phys. Chem. B* **1999**, *103*, 8726–8731.

(23) Boulmedais, F.; Schwinté, P.; Gergely, C.; Voegel, J.-C.; Schaaf, P. *Langmuir* **2002**, *18*, 4523–4525.

(24) Picart, C.; Mutterer, J.; Richert, L.; Luo, Y.; Prestwich, G. D.; Schaaf, P.; Vogel, J.-C.; Lavalle, Ph. *Proc. Natl. Acad. Sci. U.S.A.* **2002**, *99*, 12531–12535.

(25) Lavalle, Ph.; Gergely, C.; Cuisinier, F. J. G.; Decher, G.; Schaaf, P.; Voegel, J. C.; Picart, C. *Macromolecules* **2002**, *35*, 4458–4465.

(26) Debreczeny, M.; Ball, V.; Boulmedais, F.; Szalontai, B.; Voegel, J.-C.; Schaaf, P. *J. Phys. Chem. B* **2003**, *107*, 12734–12739.

(27) Boulmedais, F.; Ball, V.; Schwinté, P.; Frisch, B.; Schaaf, P.; Voegel, J.-C. *Langmuir* **2003**, *19*, 440–445.

(28) Boulmedais, F.; Bozonnet, M.; Schwinté, P.; Voegel, J.-C.; Schaaf, P. *Langmuir* **2003**, *19*, 9873–9882.

(29) Rmaile, H. H.; Schlenoff, J. B. *J. Am. Chem. Soc.* **2003**, *125*, 6602–6603.

(30) Grigsby, J. J.; Blanch, H. W.; Prausnitz, J. M. *Biophys. Chem.* **2002**, *99*, 107–116.

(31) Rosenheck, K.; Doty, P. *Proc. Natl. Acad. Sci. U.S.A.* **1961**, *47*, 1775–1785.

(32) Sreerama, N.; Woody, R. W. *Anal. Biochem.* **2000**, *287*, 252–260.

Table 1. Secondary Structure Content as a Function of pH and Charge Per Unit Length^a

PLGA	pH 4.2 (helix)				pH 7.3 (coil)			
	α helix	β sheet	β turn	coil	α helix	β sheet	β turn	coil
CONTINLL	0.882	0.013	0.000	0.106	0.138	0.240	0.249	0.373
SELCON3	0.809	0.013	0.051	0.151	0.170	0.283	0.213	0.301
CDSSTR	0.759	0.129	0.053	0.063	0.015	0.335	0.231	0.407
best estimate	0.82 ± 0.06	0.05 ± 0.07	0.03 ± 0.03	0.11 ± 0.04	0.11 ± 0.08	0.29 ± 0.05	0.23 ± 0.02	0.36 ± 0.05
PLL	pH 7.3 (coil)				pH 10.5 (helix)			
CONTINLL	0.220	0.103	0.298	0.379	0.633	0.016	0.107	0.244
SELCON3	0.005	0.037	0.279	0.715	0.464	0.081	0.215	0.254
CDSSTR	-0.022	0.375	0.229	0.379	0.757	0.052	0.036	0.151
best estimate	0.07 ± 0.13	0.17 ± 0.18	0.27 ± 0.04	0.49 ± 0.19	0.62 ± 0.15	0.05 ± 0.03	0.12 ± 0.09	0.22 ± 0.06

^a In each case the best estimate is the average of the computed percentage of a secondary structure type. The confidence interval is given by the sample standard deviation.

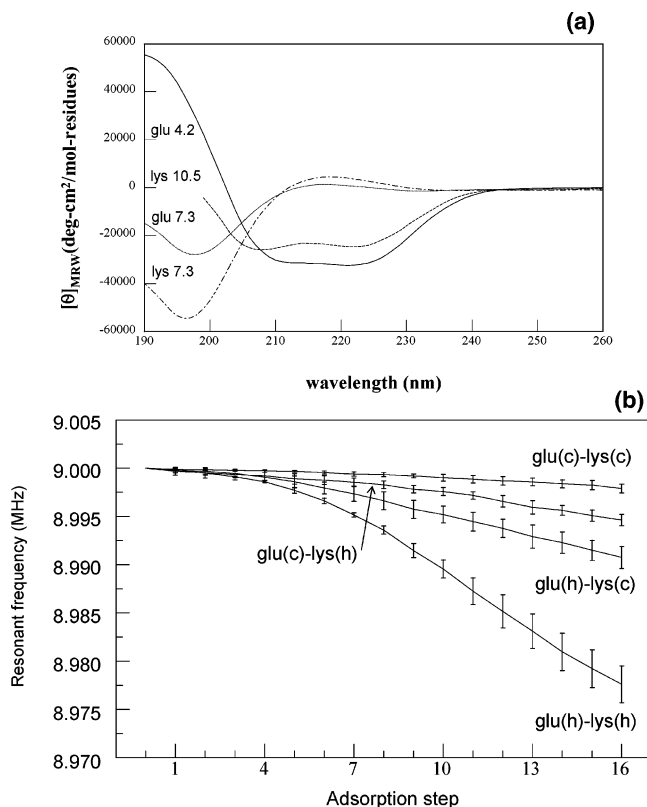


Figure 1. Effect of polymer charge per unit length on adsorption of PLGA and PLL. Both polymers had an average molecular mass of ca. 84 kDa. (a) Effect of pH on far-UV CD spectrum with minor smoothing of curves. Mean molar residue ellipticity ($\text{deg}\cdot\text{cm}^2\cdot\text{mol}^{-1}\cdot\text{residue}^{-1}$) is plotted against wavelength (nm). There are large negative Cotton effects near 195 nm in the coil state (c) and in the range 210–225 nm in the helical state (h). This shows that PLGA and PLL are substantially helical at pH 4.2 and 10.5, respectively, and both polypeptides are substantially coil-like at pH 7.3. (b) Adsorption as a function of pH and secondary structure content, monitored by QCM. Resonant frequency (MHz) is plotted against adsorption cycle. The value 8.975 MHz corresponds to a mass increment of 22 μg . The data points represent the mean value of three independent trials; the errors bars are sample standard deviations. Average frequency shift per adsorption step correlates with secondary structure content. The order in terms of increasing average frequency shift per adsorption cycle is PLGA(c)-PLL(c), PLGA(c)-PLL(h), PLGA(h)-PLL(c), and PLGA(h)-PLL(h).

than the less-ordered but more highly charged one, at low I .

Ionic Strength and Conformation. Figure 2a presents CD spectra of PLGA and PLL at pH 7.4, where $\lambda = 1$, in the absence of salt (as in Figure 1a) and at 1 M NaCl. Similar spectra were obtained throughout this concentra-

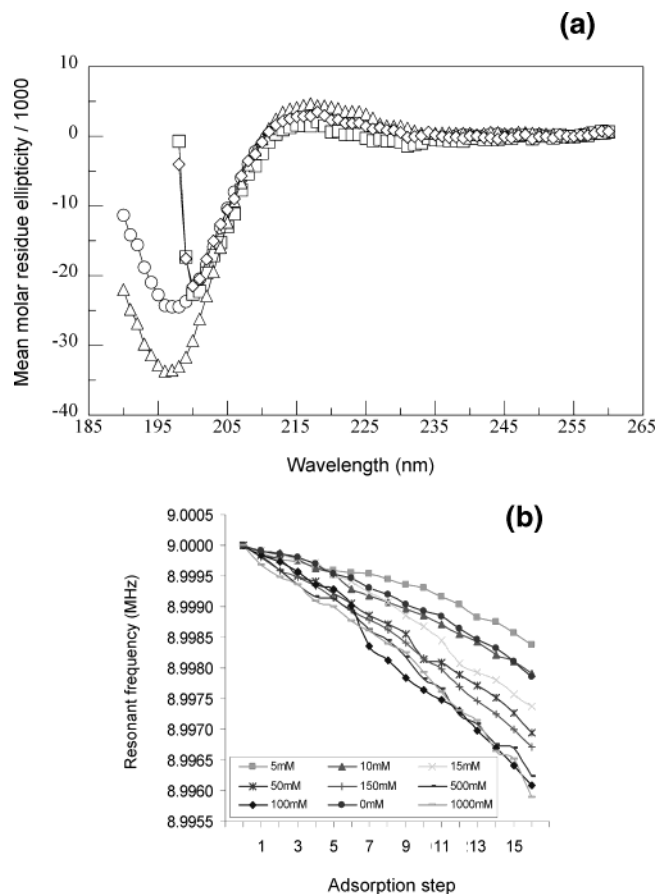


Figure 2. Effect of ionic strength on adsorption of PLGA and PLL. Both polymers have an average molecular mass of ca. 84 kDa and $\lambda = 1$. (a) Effect of salt concentration on far-UV CD spectrum. Data are shown for NaCl at 0 (PLGA, circles; PLL, triangles) and 1 M (PLGA, diamonds; PLL, squares). Mean molar residue ellipticity ($\text{deg}\cdot\text{cm}^2\cdot\text{mol}^{-1}\cdot\text{residue}^{-1}$) is plotted against wavelength (nm). (b) Adsorption as a function of I and secondary structure content, monitored by QCM. Resonant frequency (MHz) is plotted against adsorption cycle. The value 8.996 MHz corresponds to a mass increment of 3.5 μg . Frequency shift varies relatively regularly with I .

tion range (not shown). The polymers are largely disordered under these conditions. Figure 2b shows that the amount of polyelectrolyte deposited per adsorption cycle increases with I . Chain length, l , was constant (the average contour length was 238 nm), and λ was maximal. The data indicate that increased adsorption must largely be due to charge screening, even if the structure of the peptides in solution and in the film might be different.

Chain Length and Conformation. Figure 3a shows CD spectra for the polymers used to study the role of contour length in LbL at pH 7.3. All polymers were largely

disordered under these conditions, but the extent of secondary structure increased with chain length (Table 2). "Small" polymers with $\lambda = 1$ showed relatively little if any adsorption at low I , as detected by QCM (Figure 3b). By contrast, a considerable amount of polyelectrolyte was deposited during the sequential adsorption of "medium" or "large" polymers, the quantity scaling with peptide mass and number of charges. Small polymers, however, did self-assemble when the oppositely-charged polymer was sufficiently long (Figure 3b and c).

Discussion

Deconvolution of a CD Spectrum. The basic principle used to estimate secondary structure fractions was that a spectrum can be decomposed into a linear combination of separate contributions, each corresponding to a different type of secondary structure. In general terms this approximation is a more valid one for peptides than proteins, as the latter often have fixed aromatic chromophores which can contribute to the spectrum in the far UV, albeit usually negligibly. A set of spectra of model polypeptides or reference proteins of known three-dimensional structure is used to determine the relative contributions of the component spectra. Several assumptions are relevant to deconvolution (e.g., ref 33): (1) contributions from individual secondary structures are additive; (2) the secondary structure content of the ensemble average of a molecule in solution is identical to that in the corresponding X-ray structure; and (3) the effect of tertiary structure on the far-UV region of the spectrum is negligible. The results of this approach in the present context are strongly corroborated by well-established reports in the scientific literature, as indicated below.

pH and Conformation. PLGA and PLL are weak polyions, meaning that the degree of ionization can vary considerably with pH. The intrinsic pK_a of the γ -carboxyl group glutamic acid is 4.3–4.5, and that of the ϵ -amino group lysine is 10.4–11.1.³⁴ Polymerization results in a shift of pK_a toward 7 in each case. The pK_a s will be different still in a polyelectrolyte multilayer film. Determination of the pK_a of the side chains of these polymers in an LbL film was beyond the scope of the present study but will be reported elsewhere.³⁵

The pH values chosen to investigate the influence of solution structure of polypeptides on LbL were 4.5, 7.3, and 10.5. A substantial average amount of helical structure requires $\lambda \ll 1$ in the absence of a helix-promoting cosolvent such as trifluoroethanol. At the extremes a sizable percentage of α helix was induced in PLGA and PLL of identical I (Figure 1a, Table 1). The spectra compare favorably with recently published ones for PLGA at pH 6 (coil) or 3 (helix) and for PLL at pH 6 (coil) or 11 (helix) (e.g., Figure 5 of ref 36) and with long-established results (e.g., Figure 1 of ref 37). Moreover, secondary structure content estimated by deconvolution of CD spectra closely resembles long-accepted values. In this work PLGA was about 80% helical in 10 mM aqueous buffer at pH 4.2, in good agreement with the pK_a of glutamic acid in proteins³⁴ and with optical rotary dispersion measurements of

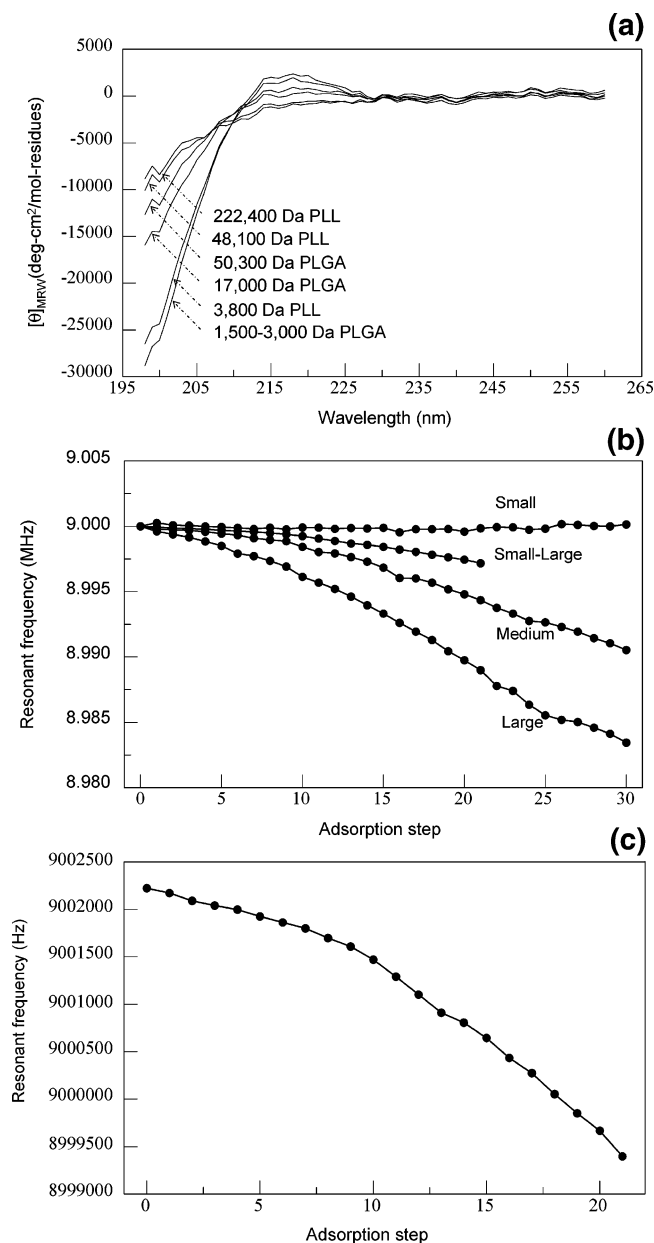


Figure 3. Effect of polymer length on adsorption of PLGA and PLL. All polymers had $\lambda = 1$. (a) Effect of chain length on far-UV CD spectrum. Data are shown for "small" PLGA, "small" PLL, "medium" PLGA, "medium" PLL, "large" PLGA, and "large" PLL. Mean molar residue ellipticity (deg·cm²·mol⁻¹·residue⁻¹) is plotted against wavelength (nm). The percentage of residues involved in secondary structure increases with chain length. (b) Adsorption as a function of I and secondary structure content, monitored by QCM. Resonant frequency (MHz) is plotted against adsorption cycle. The value 8.980 MHz corresponds to a mass increment of 17 μ g. Average frequency shift per adsorption cycle depends significantly on I . The pairs of polymers used were "small" PLGA and "small" PLL, "medium" PLGA and "medium" PLL, "large" PLGA and "large" PLL, and "small" PLGA and "large" PLL. The amount of material deposited increases with chain length. (c) Adsorption of "small" PLGA and "large" PLL, monitored by QCM. Resonant frequency (Hz) is plotted against adsorption cycle. The overall observed frequency shift corresponds to a mass increment of 2.5 μ g. The amount of material deposited per adsorption cycle is approximately independent of chain length.

Fasman et al.,³⁸ who reported 99% helix in water, pH 4.88 at 20 °C for a molecular weight of 58 or 76 kDa, and 73%

(33) Sreerama, N.; Venyaminov, S. Yu.; Woody, R. W. *Anal. Biochem.* **2000**, *287*, 243–251.

(34) Creighton, T. E. *Proteins: Structures and Molecular Properties*, 2nd ed.; Freeman: New York, 1993; p 6.

(35) Zhi, Z.-L.; Haynie, D. T. Manuscript in preparation.

(36) Muller, M.; Kessler, B.; Lunkwitz, K. *J. Phys. Chem. B* **2003**, *107*, 8189–8197.

(37) Greenfield, N.; Fasman, G. D. *Biochemistry* **1969**, *8*, 4108–4115.

(38) Fasman, G. D.; Lindblow, C.; Bodenheimer, E. *Biochemistry* **1964**, *3*, 155–166.

Table 2. Secondary Structure Content as a Function of Polymer Length^a

	PLGA			PLL		
	"small"	"medium"	"large"	"small"	"medium"	"large"
α helix	0.16 \pm 0.01	0.11 \pm 0.1	0.17 \pm 0.03	0.09 \pm 0.02	0.12 \pm 0.09	0.22 \pm 0.01
β sheet	0.15 \pm 0.10	0.19 \pm 0.1	0.20 \pm 0.07	0.28 \pm 0.04	0.20 \pm 0.14	0.22 \pm 0.01
β turn	0.26 \pm 0.03	0.27 \pm 0.02	0.25 \pm 0.01	0.25 \pm 0.02	0.25 \pm 0.03	0.25 \pm 0.01
coil	0.43 \pm 0.08	0.42 \pm 0.14	0.37 \pm 0.03	0.38 \pm 0.05	0.43 \pm 0.06	0.30 \pm 0.01

^a In each case only the best estimate is shown, computed as in Table 1. The confidence interval is given by the sample standard deviation.

helix in 0.2 M NaCl at the same pH and temperature (cf. Table 2 of the reference). PLL was about 60% helical in 10 mM aqueous buffer at pH 10.5 (Table 1 of this work). This agrees well with the pK_a of lysine in proteins³⁴ and with circular dichroism measurements of Greenfield and Fasman³⁷ at pH 11.1 and 22 °C for a molecular weight of 120 000 kDa (cf Table 1 and Figure 2 of ref 37); PLL is over 95% helical under these conditions. PLGA and PLL have relatively little helical content at neutral pH and low I , but some β sheet will be present (ref 39 and Table 1 of this work).

Other researchers who have sought to understand the relationship between polypeptide secondary structure and multilayer film assembly have reported a substantially lower helical content for these peptides in aqueous solution (25 mM MES, 25 mM Tris, 0.1 mM NaCl, 99.9% D₂O).^{23,28} In these cases, however, analysis was based on deconvolution analysis of Fourier transform infrared spectroscopy (FTIR) data. The results were as follows: PLGA pH 7.4 (coil), 58% coil, 38% turn, 4% helix; PLGA pH 4.4 (helix), 66% coil, 16% turn, 18% α helix; PLL pH 7.4 (coil), 62% coil, 30% turn, 8% α helix; PLL pH 10.4 (helix), 64% coil, 30% turn, 6% α helix (cf. Table 1 of ref 28).

It would appear that CD provides a more accurate means of determining secondary structure content than FTIR. While there are obvious potential advantages to the great sensitivity of infrared absorbance bands to the local microenvironment of different structural groups, notably, α helix and β sheet, unique adsorption band assignments are often difficult (e.g., refs 40, 41). Helical proteins associated with a membrane, for example, show an amide I band in the range 1656–1658 cm⁻¹, whereas this band occurs at 1650–1655 cm⁻¹ in soluble proteins and 1644 cm⁻¹ for solvent-exposed helices in D₂O. Moreover, the amide I absorbance bands of α helices and β sheets are inherently broad, 16–20 cm⁻¹, and the overlap between them significant. The situation is not substantially improved by collecting spectra at high resolution. Because of this, it is generally acknowledged that there is no simple way to correlate FTIR spectra of polypeptides with secondary structure content. This will be all the more true of polypeptides adsorbed to a surface or in a multilayer film than in solution. FTIR, however, can be a powerful tool for analysis of secondary structure when used in combination with other methods, notably CD.^{42–44}

In the helical state of PLGA or PLL, i.e., the vicinity of the pK_a , the total number of charges will be fluctuating. Each helix is rigid. Many small helices are present in a long peptide at any instant; however, their positions

fluctuate rapidly.⁴⁵ Counterions are relatively mobile. Overall molecular structure may be less rigid in the helical state than when $\lambda = 1$, at least at low I . This may be pertinent to the relatively large extent of adsorption of PLL and PLGA in the helical conformation. A considerable degree of induction or rigidifying of structure must occur on polypeptide adsorption.

Figure 1b shows QCM data for PLGA/PLL thin film assembly under all combinations of the conditions shown in Figure 1a. The amount of material deposited per adsorption cycle correlates with structural properties of the polypeptides in solution. At pH 7.3, when both polypeptides were in a largely random conformation, relatively little material was deposited per adsorption step. The thickness of these films can be estimated from a report involving optical waveguide light mode spectroscopy (OWLS) measurements: the thickness of a PLGA/PLL film fabricated in 25 mM Tris, 25 mM MES, pH 7.4, and 0.1 M NaCl was about 140 nm for 7 bilayers and 70 nm for 4 bilayers, the first 20 nm corresponding to 5 "precursor" layers, one of poly(ethyleneimine) (PEI) and two bilayers of poly(sodium 4-styrene-sulfonate) (PSS) and PAH (cf Figure 3 of ref 28). Lavalle et al. reported a film thickness of about 65 nm for PEI:(PLL/PLGA)₄ and 280 nm for PEI:(PLL/PLGA)₈ following assembly in 25 mM MES, 25 mM Tris, pH 7.4, and 0.1 M NaCl (cf. Figure 2 of ref 25). Such data, when compared to the QCM results reported here, could be used to estimate a multiplicative factor to translate a frequency shift measurement into a film thickness. It would be better, however, to make a more direct measurement, e.g., using ellipsometry.

Figure 1b also shows that more material was deposited when at least one peptide was in a helical conformation, and deposition was greatest when both peptides were helical. This resembles the so-called anomalous adsorption of polyelectrolyte layers described by Rubner and co-workers. In their case the polyelectrolyte charge density was fixed, the polyelectrolytes were not structured in solution, and the surface charge density varied⁴⁶ (see also refs 18 and 19). Qualitatively similar results are reported by Boulmedais et al.,²⁸ who monitored changes in multilayer film thickness when both PLGA and PLL were dissolved in aqueous solution at a pH value in the range 1.5–11.3. They found that the thickness of 7 bilayers was about 400 nm at pH 10.4, 200 nm at pH 11.3, 150 nm at pH 7.4, 120 nm at pH 4.4, and of 3 bilayers 175 nm at pH 1.5 (cf Figure 1 of the reference). In all cases the first five layers were PEI:(PSS/PAH)₂, the thickness ranging from 10 (pH 4.4) to 60 nm (pH 1.5). It is remarkable that pH 4.4 gave such a thin film and pH 1.5 such a thick one. The QCM work reported here did not involve precursor layers and did investigate deposition of helical peptides onto helical peptides.

It could be argued that deposition of polypeptide was least when λ was maximal and greatest when λ was

(39) Alder, A. J.; Greenfield, N. J.; Fasman, G. D. *Methods Enzymol.* **1973**, *27*, 675–735.

(40) Chapman, D.; Jackson, M.; Haris, P. I. *Biochem. Soc. Trans.* **1989**, *17*, 617–619.

(41) Jackson, M.; Haris, P. I.; Chapman, D. *Biochemistry* **1991**, *30*, 9681–9686.

(42) Kelly, S. M.; Price, N. C. *Biochim. Biophys. Acta* **1997**, *1338*, 161–185.

(43) Greenfield, N. J. *Anal. Biochem.* **1996**, *235*, 1–10.

(44) Bloemendal, M.; Johnson, W. C., Jr. *Pharm. Biotechnol.* **1995**, *7*, 65–100.

(45) Poland, D.; Scheraga, H. A. *Theory of Helix-Coil Transitions in Biopolymers*; Academic: New York, 1970.

(46) Park, S. Y.; Barrett, S. J.; Rubner, M. F.; Mayes, A. M. *Macromolecules* **2001**, *34*, 3384–3388.

relatively small. This would suggest that thin layers are formed when λ is large (electrostatic LbL) and thick layers when λ is small (LbL governed by "secondary interactions" and low polymer solubility; reviewed in ref 47). Nevertheless, it could hardly be supposed that structural features of a polypeptide in solution are irrelevant to the adsorption process nor is it thinkable that all structural features of a polypeptide in solution are "lost" on adsorption, even if rearrangements might occur as the free energy of the film is minimized during a slow kinetic process.

More material was deposited for PLGA than PLL in the helical state (Figure 1b), even though $\lambda \approx 0.5$ for each. The data in Table 1 suggest that more than 80% of PLGA was helical at pH 4.2, while PLL was about 60% helix and 20% coil; β -sheet content was about 10% in each case. The lysine side chain is more hydrophobic than the glutamic acid side chain; there are four methylene groups in lysine and two in glutamic acid. The polar accessible surface area of glutamic acid, however, is about 2-fold larger than that of lysine.⁴⁸ This suggests that PLGA will generally be the more soluble of the two polypeptides in aqueous solution, not the less soluble, contrary to the interpretation that hydrophobic interactions drive assembly when the peptides are largely helical.

There is no obvious reason to expect PLGA to form better hydrogen bonds or more of them per unit length than PLL. The hydrogen-bonding potential of the polypeptide backbone, which comprises amine hydrogen donors and carbonyl oxygen acceptors, is identical in these polymers. Hydrogen bonds do play a crucial role in formation of an α helix or a β sheet. The hydrogen-bonding potential of the polypeptide backbone can be fully realized in both types of structure, though the second law of thermodynamics will require the presence of at least some random structure in a polypeptide of any length under any solution conditions in the liquid state.⁴⁵

In an α helix, all hydrogen bonds are intramolecular ones, formed between residues i and $i + 4$; all hydrogen-bond donors and acceptors are in "local" residues (e.g., ref 49). Residue side chains are perpendicular to the helix axis. In a β sheet, hydrogen bonds are formed between "nonlocal" residues. Both intra- and intermolecular bonds are possible, and two β strands can form either a "parallel" or an "antiparallel" β sheet, depending on the relative directionality of the strands. An "antiparallel" β sheet is more thermostable than a parallel one, all else being equal, owing to greater favorability of geometry of hydrogen-bond formation. Regardless of β -sheet type, the side chains are perpendicular to the plane of the sheet. The possibility, then, of forming a variety of β structures that are fully hydrogen bonded provides degrees of freedom favoring β -sheet formation over α helix formation. Obviously the number of hydrogen-bond donors and acceptors available for rapid intermolecular hydrogen bonding on adsorption will be low when the degree of secondary structure formation in solution is high.

Entropy change could be a significant determinant of the extent of polypeptide adsorption. The overall conformational change during film formation may be large or small when there is a significant amount of α helix or β

sheet present in solution; the extent of conformational change may depend on the process. Largely unstructured molecules might behave rather differently. There are more rotational degrees of freedom in the side chain of lysine than glutamate. In view of this, helical PLGA may be more favored for adsorption than helical PLL because of a smaller reduction in side-chain entropy. In any case, the data indicate that differences in helix content in solution correlate with differences in adsorption behavior.

The effect on film structure of alternating the pH of solution into which the film is dipped was not determined in this study. For instance, it is possible that the helical structure of PLGA deposited at pH 4.2 does not persist during adsorption of a layer of helical PLL at pH 10.5. If structural changes do occur in the film during each adsorption cycle, it is possible that this plays a role in determining physical properties of the final product, for instance, film thickness and stability in a harsh environment.

Ionic Strength and Conformation. Salt influences the structure of a polypeptide in aqueous solution. Figure 2a shows how the spectrum of PLGA and of PLL changes on addition of NaCl at pH 7.4. In these experiments $\lambda \approx 1$ and I was the same for both polymers. Deconvolution indicates that PLGA and PLL were largely in disordered conformations at pH 7.4, both in the absence of salt (as in Figure 1a) and at 1 M NaCl. It is also evident from Figure 2a that a structural change occurred in the range 0–1 M, but its precise character was not clarified by deconvolution (data not shown). Some types of polyelectrolyte form a coil structure in the presence of counterions, due to the screening of monomer charges (e.g., refs 50 and 51), and this may influence the adsorption process.

The amount of polymer deposited per adsorption step increased with I (Figure 2b). Similar behavior is exhibited by polyelectrolytes such as PSS and PAH (ref 16 and references therein). The effective value of λ must decrease with I due to Debye screening, so in this case the molecular cause of increased adsorption at high I would appear to be increased relative importance of "secondary" interactions and possible effects of salt on interactions in the film between oppositely charged polymers. Some of the observed frequency shift might arise from the entrapment of counterions in the film.

Chain Length and Conformation. These experiments were done at pH 7.3, where $\lambda \approx 1$, and the only contributors to I were the polymers and counterions. The concentration of charged side chains and of counterions was constant, regardless of chain length. The persistence length of the polymers was expected to be relatively large under these conditions. The molecular mass of the adsorbing polypeptides ranged over 2 orders of magnitude. Figure 3a and Table 2 show that the extent of structure formation in solution depended on chain length.⁴⁵

Multilayer thin film assembly was achieved when the oppositely-charged polypeptides were relatively long but not when the polypeptides were relatively short (Figure 3b). This indicates that the ability of polypeptides to self-assemble in electrostatic LBL is not merely a function of I . Moreover, it resembles the finding that oppositely-charged polyions must have ~ 20 or more charged groups to form a complex in aqueous solution (e.g., refs 52 and 53). Furthermore, it suggests that when I is small, the entropic cost of fixing the translational degrees of freedom

(47) Oliveira, O. N.; He, J.-A.; Zucolotto, V.; Balasubramanian, S.; Li, L.; Nalwa, H. S.; Kumar, J.; Tripathy, S. K. In *Handbook of Polyelectrolytes and their Applications: Polyelectrolyte-based Multilayers, Self-assemblies and Nanostructures*; American Scientific: Stevenson Ranch, CA, 2002; Vol. 1, pp 1–37.

(48) Millar, S.; Janin, J.; Les, A. M.; Chothia, C. *J. Mol. Biol.* **1987**, *196*, 641–656.

(49) Cantor, C. R.; Schimmel, P. R. *Biophysical Chemistry. Part I: The Conformation of Biological Macromolecules*; Freeman: New York, 1980.

(50) Odijk, T. J. *Polym. Sci. (Polym. Phys. Ed.)* **1977**, *15*, 477–483.

(51) Skolnick, J.; Fixman, M. *Macromolecules* **1977**, *10*, 944–948.

(52) Kabanov, V.; Zevin, A. *Pure Appl. Chem.* **1984**, *56*, 343–354.

(53) Kabanov, V. *Polym. Sci.* **1994**, *36*, 143–156.

of the center of mass of a molecule may outweigh the favorability of the electrostatic interactions it can make in a film. This is consistent with the possibility that formation of soluble polyanion–polycation complexes at the solid–liquid interface may lead to deposited polypeptide leeching off the surface, resulting in negligible accumulation of material on the substrate over a number of dipping cycles (Figure 3b). The results and interpretation are consistent with recent work involving different polyelectrolytes.⁵⁴

Figure 3c shows an expanded view of the “small”–“large” assembly. The apparent mass deposited per adsorption cycle, Δm , was practically independent of I . There was an insignificant difference in frequency shift on adsorption of the small polymer or the large one. It follows that the number density of adsorbed molecules is inversely related to I when $\lambda \approx 1$ and I is low.

The underlying mechanism of the observed length dependence of adsorption might be complex, as the frequency shift for a given number of bilayers does not correlate simply with any obvious function of the mass of the positive and negative polymers. The contribution made to I by polymer counterions is not likely to be the cause of the observed length dependence, as the concentration of charged residues and of counterions was the same in all experiments.

It has been mentioned that hydrogen bonds are known to play a role in multilayer film assembly (e.g., refs 9 and 20). Such research has shown, for example, that the amount of adsorbed polyaniline is larger in LbL films assembled by hydrogen bonding than ionic interactions. The hydrogen-bonding potential of PLGA to PLL, however, in the absence of a structural change on adsorption, must decrease with chain length because the degree of departure from a completely disordered conformation increases moderately with chain length (Figure 3c and Table 2). While this does not necessarily imply that intermolecular hydrogen-bond formation plays no role in polypeptide LbL, it suggests that the situation is rather complex and that the average content of secondary structure in solution might influence polypeptide adsorption to a significant degree.

“Long” peptides can form a variety of secondary structures in solution: α -helix, 3_{10} -helix, other types of helix, parallel β -sheet, antiparallel β -sheet, etc. All such structures are stabilized by hydrogen bonds. PLL can form a substantial amount of relatively rigid β -structure in aqueous solution (e.g., refs 55 and 56). Stability of this structure may depend in part on hydrophobic interactions. The probability of secondary structure formation in long polypeptides in aqueous solution will depend on I , pH, I , and distribution of charge. Long peptides can also condense into irregular structures of varying density, which may or may not feature secondary structure. By contrast, short peptides, particularly ones with a high charge density, must pay a relatively high entropic cost to form secondary structure (i.e., thermodynamically favorable hydrogen bonds), particularly at moderate values of pH or I . At equilibrium, short polypeptides are likely to be relatively rodlike in solution and long polypeptides are likely to adopt a broad range of conformations. This suggests how the adsorption process might depend on polymer structure.

Conclusion

PLGA and PLL have been used to investigate the relationship between molecular structure in solution and adsorption behavior. These polymers can be used to fabricate multilayer thin films by LbL, as discussed previously by Voegel, Schaaf, and colleagues^{12,23–28} and by Schlenoff and colleagues.²⁹ The present work has provided new insight on the nature of polypeptide LbL by combining accurate determination of the secondary structure of the polymers in solution with accurate determination of the mass of polymer deposited onto a surface.

QCM enabled quantitative determination of polypeptide adsorption to previously formed layers of oppositely charged polypeptides. CD analysis revealed the type and quantity of secondary structure of polypeptide chains in solution. Combining data from these methods has shown that the extent of adsorption in LbL scales with the extent of secondary structure in solution. This research has also added CD to the “toolbox” of methods for analysis of multilayer films; CD is better suited to determination of secondary structure in polypeptides in solution and in films⁵⁷ than FTIR. The approach taken in this work could advance experimental and theoretical studies on adsorption of semi-flexible charged polymers on an oppositely charged surface and provide a basis for technological exploitation of polypeptide LbL.

The polypeptide adsorption process would appear to be driven by a balance of electrostatic repulsion between subunits in the same molecule, the effect of such repulsion on secondary structure formation and chain stiffness, electrostatic attraction between the polymer and the surface to which it adsorbs, hydrophobic interactions, and the entropic cost of reducing the translational and conformational degrees of freedom of the polypeptide chain. Hydrogen-bond formation also may be important to polypeptide multilayer formation, but in all experiments discussed here intramolecular hydrogen bonding in solution (CD) correlated with the amount of material adsorbed (QCM)—the opposite of what would be expected if hydrogen bonds played such an important role in film stabilization, unless the secondary structure evident in solution is lost on adsorption. Further research is needed to determine the relative importance of each contribution in polypeptide LbL. It also remains to be determined whether the structure exhibited by the polypeptides in solution will actually be maintained in a multilayer film, as reported values for secondary structure content based on deconvolution of FTIR spectra cannot be considered accurate. It seems nonetheless clear, however, that the simple models studied here can reveal a good deal about the nature of polyelectrolyte adsorption and suggest means of developing polypeptide-based thin films and coatings.

Future prospects for the fabrication of polypeptide thin films, coatings, and microcapsules seem especially promising. Indeed, there are 20 usual amino acid types and a huge number of nonnatural amino acids; the number of possible polypeptide sequences is effectively unlimited; peptide synthesis can be achieved either abiotically, using a peptide synthesizer, or by genetic modification of a suitable host organism; and extensive research has been done on the use of proteins in the fabrication of films and coatings for applications in food science, pharmaceuticals, waste disposal, and other applications.⁵⁸ The ability to

(54) Sui, Z.; Salloum, D.; Schlenoff, J. B. *Langmuir* **2003**, *19*, 2491–2495.

(55) Sarkar, P. K.; Doty, P. *Proc. Natl Acad. Sci. U.S.A.* **1966**, *55*, 981–989.

(56) Townend, R.; Kumosinski, T. F.; Timasheff, S. N.; Fasman, G. D.; Davidson, B. *Biochem. Biophys. Res. Commun.* **1966**, *23*, 163–169.

(57) Stevens, L.; Townend, R.; Timasheff, S. N.; Fasman, G. D.; Potter, J. *Biochemistry* **1968**, *7*, 3717–3720.

(58) *Protein-based Films and Coatings*; Gennadios, A., Ed.; CRC Press: Boca Raton, FL, 2002.

design and fabricate polypeptides could be of substantial value for the future development of such films, coatings, and microcapsules made of these materials.

Acknowledgment. We thank Bingyun Li, Zheng-liang Zhi, Yuri Lvov, Gleb Sukhorukov, and Michael Rubner for discussions and anonymous reviewers for helpful

comments. This work was supported by a seed grant from the Center for Entrepreneurship and Information Technology and an enhancement grant from the Louisiana Space Consortium (Louisiana NASA EPSCoR, project R127172).

LA036330P